Int. J. Nanoelectronics and Materials **3** (2010) 53-67

# Linear and nonlinear optical susceptibilities in some ferroelectrics: Ab-initio calculation

Harun Akkus[1], Suleyman Cabuk[1*], Amirullah M. Mamedov[2♦]

[1]*Physics Department, Yuzuncu Yil University, Van, Turkey.*
[2]*Physics Department, Cukurova University, Adana, Turkey.*

## Abstract

We present a first principles calculations of the second-order optical response functions as well as the dielectric function for $ABO_3$ (A=K, Li, Ba; B=Ti, Ta, Nb) and $A^5B^6C^7$ ( A=Sb; B=S, Se; C=I, Br ) ferroelectrics. Specially, we evaluate the dielectric function $\varepsilon(\omega)=\varepsilon_1(\omega)-i\varepsilon_2(\omega)$ and the second harmonic generation response coefficient $\chi^{(2)}(-2\omega, \omega, \omega, \omega)$ over a large frequency range. The electronic linear electro-optic susceptibility $\chi^{(2)}(-\omega, \omega, \omega, 0)$ is also evaluated below band gap. These results are based on the series of self-consistent LDA calculations within DFT.

**Keywords:** Ferroelectrics, Optical susceptibility, ab initio methods.
**PACS:** 77.22-d, 71.20.-b, 74.20.Pq.

## 1. Introduction

Nowadays, nonlinear optics has developed a field of major study because of rapid advance in photonics [1]. Nonlinear optical techniques have been applied to many diverse disciplines such as

*) For correspondence; Email: scabuk@cu.edu.tr.
♦) For correspondence; Email: mamedov@cu.edu.tr.

condensed matter physics, medicine and chemical dynamics. The development of new advanced nonlinear optical materials for special applications is a crucial importance in technical areas such as optical signal processing and computing, acousto-optic devices and artificial neuro-network implementation. However, there is comparatively a much smaller effort to understand the nonlinear optical process in these materials at the microscopic level. Theoretical understanding on the factor that controls the figure of merit is extremely important in improving the existing electrooptic (EO) materials, and in the search for new ones [2].

Even though there exist a number of calculations for the electronic band structure and optical properties using different methods [3-10]. There is a large variation in the energy gaps, suggesting that the energy band gap depends on the method of the energy spectra calculation. We therefore thought it was worthwhile to perform calculations using density functional theory (DFT) in the local density approximation (LDA) expressions, as implemented within ABINIT package [8] the following convention.

In this paper, we describe details calculations of the linear and nonlinear optical properties, includes second harmonic generation response coefficient $\chi^{(2)}(-2w, w, w)$ over a large frequency range for some $ABO_3$ (A= Ba, K, Li, B=Ti, Ta, Nb) and $A^5B^6C^7$ ( A=Sb, B=S, C=I, Br ) ferroelectrics.

## 2. Computational details

The nonlinear optical properties of ferroelectrics were theoretically studied by means of first principles calculations in the framework of DFT and based on the LDA[11] as implemented in the ABINIT code[8,12]. The self–consistent norm-conserving pseudopotentials are generated using Troullier-Martins scheme [13] which is included in the Perdew-Wang [14] scheme as parameterized by Ceperly and Alder [15]. The Brillouin zone was sampled using a 6 x 6 x 6 the Monkhorst-Pack[16] mesh of special k points. Rhombohedral position coordinates of $LiNbO_3$ and $LiTaO_3$ using both experimental value [17, 18] were calculated to relate to the hexagonal coordinates given in the literature by the transformation [19]. The coordinates of $KNbO_3$ [20] and $BaTiO_3$[21] are reported in Table 1.

All calculations of $ABO_3$ and $A^5B^6C^7$ have been used with the experimental lattice constants and atomic positions. The lattice constants and atomic positions are given in Table 1. The coordinates of the other atoms can easily be obtained by using the symmetry operations of the space groups. These parameters were necessary to obtain converged results in the nonlinear optical properties and phonons data at Γ point of the Brillouin zone.

Table 1: The lattice parameters and atomic positions in $ABO_3$

| Phase | Space | Lattice Group Parameters (Å) | Atom | Position |
|---|---|---|---|---|
| $LiNbO_3$ Ferroelectric (Rhombohedral) | R3c | a = b = c=5.4944 | Li<br>Nb<br>O | (0.2829, 0.2829, 0.2829)<br>(0.0000, 0.0000, 0.0000)<br>(0.1139, 0.3601,-0.2799) |
| $LiTaO_3$ Ferroelectric (Rhombohedral) | R3c | a = b = c=5.4740 | Li<br>Ta<br>O | (0.2790, 0.2790, 0.2790)<br>(0.0000, 0.0000, 0.0000)<br>(0.1188, 0.3622,-0.2749) |
| $KNbO_3$ Ferroelectric (Tetragonal) | P4mm | a=b=3.997, c=4.0630 | K<br>Nb<br>O(1)<br>O(2) | (0.000, 0.000, 0.023)<br>(0.500, 0.500, 0.500)<br>(0.500, 0.500, 0.040)<br>(0.500, 0.000, 0.542) |
| $BaTiO_3$ Ferroelectric (Tetragonal) | P4mm | a=b=3.9909, c=4.0352 | Ba<br>Ti<br>O(1)<br>O(2) | (0.0000, 0.0000, 0.0000)<br>(0.5000, 0.5000, 0.5224)<br>(0.5000, 0.5000,-0.0244)<br>(0.5000, 0.0000, 0.4895) |
| SbSBr Ferroelectric (Orthorombic) | Pnma | a=8.168, b=9.7, c=3.942 | Sb<br>S<br>Br | (0.1235, 0.1321, 0.2777)<br>(0.8370, 0.0486, 0.2585)<br>(0.5135, 0.8231, 0.2500) |
| SbSI Ferroelectric (Orthorombic) | Pnma | a=8.52, b=10.13, c=4.10 | Sb<br>S<br>I | (0.119, 0.124, 0.298)<br>(0.843, 0.049, 0.261)<br>(0.508, 0.828, 0.250) |

## 3. Linear and nonlinear optical response

### 3.1 Linear optical response

It is well known that the effect of the electric field vector, $E(\omega)$, of the incoming light is to polarize the material. In an insulator the polarization can be expressed as a Taylor expansion of the $E(\omega)$

$$P^i(\omega) = P_s^i + \sum_{j=1}^{3} \chi_{ij}^{(1)}(-\omega,\omega)E^j(\omega) + \sum_{j,l=1}^{3} \chi_{ijl}^{(2)} E^j(\omega)E^l(\omega) + \ldots \qquad (1)$$

where $P_s^i$ is the spontaneous polarization, $\chi_{ij}^{(1)}$ is the linear optical susceptibility tensor [22 ]. $\chi_{ijl}^{(2)}$ the second-order nonlinear susceptibility tensor and will discusses in sec.4. The dielectric function $\varepsilon_{ij}(\omega) = [1 + 4\pi\chi_{ij}^{(1)}(-\omega,\omega)]$ and the imaginary part of $\varepsilon_{ij}(\omega)$, $\varepsilon_2^{ij}(\omega)$ is given by

$$\varepsilon_2^{ij}(\omega) = \frac{e^2}{\hbar\pi} \sum_{nm} \int d\vec{K} f_{nm}(\vec{K}) \frac{v_{nm}^i(\vec{K}) v_{mn}^j(K)}{\omega_{mn}^2} \delta(\omega - \omega_{mn}(K)) \qquad (2)$$

The real part of $\varepsilon_{ij}(\omega), \varepsilon_1^{ij}(\omega)$, can be obtained by using Kramers-Kronig transformation

$$\varepsilon_1^{ij}(\omega) - 1 = \frac{2}{\pi} \mathrm{P} \int_0^{\infty} \frac{\omega' \varepsilon_2^{ij}(\omega')}{\omega'^2 - \omega^2} d\omega' \qquad (3)$$

As the Kohn-Sham equations only determine the ground-state properties, hence the unoccupied conduction bands have no physical significance. If they are used as single-particle states in optical calculation of dielectric, a band gap problem comes into existence: The absorption starts at a too low energy [23]. In order to remove the deficiency the many-body effects must be included in calculations of response functions. In order to take into account the self-energy effect, generally used the scissors approximation [23]. In the calculation of the optical response in present work we have used the standard expression for $\varepsilon_{ij}(\omega)$ (see Eq.2 and 3).

### 3.2 Nonlinear response

The general expression of the nonlinear optical susceptibility depends on the frequencies of the $E(\omega)$. Therefore, in present context

of the (2n+1) theorem applied within the LDA to DFT we get expression for the second order susceptibility [22-25]. As the sum of the three physically different contributions

$$\chi^{(2)}_{ij\beta\gamma\beta j}(-\omega,-\omega,\omega,\omega)=\chi''_{ijl\beta\gamma\beta j}(-\omega,-\omega,\omega,\omega)+\eta''_{ijl\beta j\beta j}(-\omega,-\omega,\omega,\omega)+i\frac{\sigma''_{ijl\beta j\beta\gamma}(-\omega,-\omega,\omega,\omega)}{\omega+\omega_{\beta\gamma}} \quad (4)$$

That includes contributions of interband and intraband transitions to the second order susceptibility. The first term in Eq.4 describes contribution of interband transitions to second order susceptibility. The second term represents the contribution of intraband transitions to second order susceptibility and the third term is the modulation of interband terms by intrabands terms. We have used this expression to calculate nonlinear response functions of ferroelectrics.

### 3.3 Principal refractive indices calculation

The principal refractive indices, $n_i$, can be computed as a square root of the eigenvalues of the optical dielectric tensor. This term is difficult to compute in practice. However, in usual ferroelectric such as $BaTiO_3$ or $KNbO_3$, the variations of $n_i$ in the paraelectric phase are small compared to their variation at the phase transition. Following ref.[22] we will neglect the thermal fluctuation and their correlations since we are interested in the variation of $n_i$ below the phase transition temperature ($T_c$) where we expect the term that describes the variatious of $\chi^{(1)}$ due to the averaged crystal lattice distortions to dominate. The linear EO effect is related to the first order change of the optical dielectric tensor induced by a static or low frequency electric field.

### 3.4 Electro-Optic tensor

The optical properties of material usually depend on external parameters such as the temperature, electric or magnetic fields or mechanical constraints (stress, strain). Now we consider the variations of the refractive index induced by a static or low-frequency electric field $E$. At linear order, these variations are described by the linear electro-optical (EO) coefficients (Pockels effect).

$$\Delta(\varepsilon^{-1})_{ij} = \sum_{k=1}^{3} r_{ijk} E_k \tag{5}$$

where $(\varepsilon^{-1})_{ij}$ is the inverse of the electronic dielectric tensor and $r_{ijk}$ the EO tensor. Within the Born-Oppenheimer approximation, the EO tensor can be expressed as the sum of the three contributions: a bare electronic part $r_{ijk}^{el}$, an ionic contribution $r_{ijk}^{ion}$ and a piezoelectric contribution $r_{ijk}^{piezo}$. The electronic part is due to an interaction of $E_k$ with the valence electrons when considering the ions artificially as clamped at their equilibrium positions. It can be computed from the nonlinear optical coefficients. As can be seen from Eq.4 $\chi_{ijl}^{(2)}$ defines the second order change of the induced polarization with respect to $E_k$. We have to transform $\Delta\varepsilon_{ij}$ to $\Delta(\varepsilon^{-1})_{ij}$ by the inverse of the zero-field electronic dielectric tensor [34].

$$\Delta(\varepsilon^{-1})_{ij} = -\sum_{m,n=1}^{3} \varepsilon_{im}^{-1} \Delta\varepsilon_{mn} \varepsilon_{nj}^{-1} \tag{6}$$

We obtain the following expression for the electronic EO tensor:

$$r_{ijk}^{el} = -8\pi \sum_{l,l'=1}^{3} (\varepsilon^{-1})_{il} \chi_{ll'k}^{(2)} (\varepsilon^{-1})_{l'j} \tag{7}$$

Eq.7 takes a simpler from when expressed in the principal axes of the crystal under investigation [34]:

$$r_{ijk}^{el} = -\frac{8\pi}{n_i^2 n_j^2}\chi_{ijk}^{(2)} \tag{8}$$

where $n_i$ coefficients are the principal refractive indices.

The origin of ionic contribution to the EO tensor is the relaxation of the atomic positions due to the applied electric field $E_k$ and the variations of the $\varepsilon_{ij}$ induced by these displacements. It can be computed from the Born effective charge $Z^*_{k,\alpha,\beta}$ and the $\partial\chi_{ij}/\partial T_{k\alpha}$ coefficients introduced in [34].

In the discussion of the EO effect, we have to specify whether we are dealing with strain-free (clamped) or stress-free (unclamped) mechanical boundary conditions. The clamped EO tensor $r_{ijk}^{\eta}$ takes into account the electronic and ionic contributions but neglects any modification of the unit cell shape due to the converse piezoelectric effect [7].

$$r_{ijk}^{\eta} = r_{ijk}^{el} + r_{ijk}^{ion} \tag{9}$$

Experimentally, it can be measured for frequencies of $E_k$ high enough to eliminate the relaxations of the crystal lattice but low enough to avoid excitations of optical phonon modes (usually above ~ $10^2$ MHz). To compute the unclamped EO tensor $r_{ijk}^{\sigma}$ we have added the piezoelectric contribution to $r_{ijk}^{\eta}$. In contrast to the dielectric tensor, the EO coefficients can either be positive or negative. The sign of these coefficients is often difficult to measure experimentally. Moreover, it depends on the choice of the Cartesian axes. The z-axis is along the direction of the spontaneous polarization and the y – axis

lies in a mirror plane. The z and y–axis are both piezoelectric. Their positive ends are chosen in the direction that becomes negative under compression. The orientation of these axes can easily be found from pure geometrical arguments. Our results are reported in the Cartesian axis where the piezoelectric coefficients $d_{22}$ and $d_{33}$ are positive. These coefficients, as well as their total and electronic part, are reported in Table 2. All EO coefficients are positive as is the case for the noncentro-symmetric phases [7], the phonon modes that have the strongest overlap with the soft mode of the paraelectric phase dominate the amplitude to the EO coefficients. Moreover, the electronic contributions are found to be quite small. All our investigation of EO coefficients of $ABO_3$ shows a good agreement and also between our results and earlier investigations.

Table 2: EO tensors (a), and Second-order nonlinear optical susceptibilities (b) for some $ABO_3$ and $A^5B^6C^7$ crystals

(a)

| Crystal | Symmetry Class | | EO coefficients x $10^{-7}$ (esu) | | | |
|---|---|---|---|---|---|---|
| | | | Electronic | Total | Exp | |
| $BaTiO_3$ | 4mm | $r_{13}$ | 0.358 | 1.653 | 3.06 | [27] |
| | | $r_{33}$ | 0.505 | 3.570 | 12.18 | [27] |
| $KNbO_3$ | 4mm | $r_{13}$ | 0.288 | 1.279 | | |
| | | $r_{33}$ | 1.029 | 5.117 | | |
| | | $r_{51}= r_{42}$ | 0.288 | 1.279 | | |
| | 3m | $r_{13}$ | 0.569 | 3.417 | | |
| | | $r_{33}$ | 0.942 | 6.276 | | |
| | | $r_{51}= r_{42}$ | 0.623 | 3.459 | | |
| | | $r_{22}$ | 0.254 | 1.333 | | |
| $LiNbO_3$ | 3c | $r_{13}$ | 0.230 | 1.756 | 2.58 | [28] |
| | | $r_{33}$ | 0.082 | 6.085 | 9.24 | [28] |
| | | $r_{51}= r_{42}$ | 0.236 | 1.879 | 8.40 | [28] |
| | | $r_{22}$ | 0.002 | 0.402 | 1.02 | [28] |
| $LiTa\ O_3$ | 3c | $r_{13}$ | 0.092 | 3.153 | 2.52 | [29] |
| | | $r_{33}$ | 0.718 | 5.151 | 0.06 | [29] |
| | | $r_{51}= r_{42}$ | 0.091 | 1.105 | 9.15 | [29] |
| | | $r_{22}$ | 0.039 | 0.132 | -6.00 | [29] |
| SbSI | mm2 | $r_{33}$ | 35 | 620 | - | |
| SbSBr | mm2 | $r_{33}$ | 98 | 910 | - | |

(b)

| Crystal | Symmetry Class | $D_{x1}$ x $10^{-7}$ (esu) | | | | |
|---|---|---|---|---|---|---|
| | | $d_{15}$ | $d_{22}$ | $d_{31}$ | $d_{33}$ | Exp |
| $BaTiO_3$ | 4mm(cal) | 2.457 | - | 2.547 | 2.885 | |
| | (exp) | 5.1 | - | 4.71 | 2.040 | [40] |
| $KNbO_3$ | 4mm (cal) | 2.190 | - | 2.190 | 5.322 | |
| | (cal) | - | - | -0.299 | -0.818 | [40] |
| | 3m (cal) | - | 1.546 | 3.465 | 4.788 | |
| | (cal) | - | 0.342 | 0.121 | 0.342 | [40] |
| $LiNbO_3$ | 3c (cal) | - | 0.013 | 1.541 | 6.877 | |
| | (exp) | - | 0.774 | -1.464 | 0.342 | [40] |
| $LiTa\ O_3$ | 3c (cal) | - | 0.221 | 0.513 | 4.114 | |
| | (exp) | - | 0.51 | -0.321 | -4.92 | [41] |
| SbSI | mm2 (cal) | - | - | - | 9.3 | |
| SbSBr | mm2 (cal) | - | - | - | 12.4 | |

## 4. Results and discussion

The calculation of nonlinear optical properties is much more complicated than the same procedure in the linear case. The difficulties concern both the numerical and the physics. The k-space integration in expression (6) has to be performed more carefully using a generalization of methods [24-26]. More conduction bands have to be taken into account to reach the same accuracy. The fact that the SHG coefficients are related to the optical transitions has remarkable consequences. First of all, we note that the equations for SHG consist of a number of resonant terms. In this sense the imaginary part, $Im\chi^{(2)}(-2\omega,\omega,\omega)$ resembles the $\epsilon_2(\omega)$ and provides a link to the band structure. The difference, however, is that whereas in $\epsilon_2(\omega)$ only the absolute value of the matrix elements squared enters, the matrix elements entering the various terms in $\chi^{(2)}$ are more varied. They are in general complex and can have any sign. Thus, $Im\chi^{(2)}(-2\omega,\omega,\omega)$ can be both positive and negative. Secondly, there appear both resonances when $2\omega$ equals a interband energy and when $\omega$ equals an interband energy. Fig. (1-2) shows the $2\omega$ and single $\omega$ resonances contributions to $Im\chi^{(2)}(-2\omega,\omega,\omega)$ compared to $\epsilon_2(\omega)$ (Fig. 6) for a number of $ABO_3$

and $A^5B^6C^7$. They clearly show a greater variation from high symmetry to lowest symmetry than the linear optic function. In some sense they resemble a modulated spectrum. Thirdly, we note that the 2ω resonances occur at half the frequency corresponding to the interband transition. Thus, the incoming light need not be as high in the UV to detect this higher lying interband transition. This is important for wide band gap materials like $ABO_3$ compounds where laser light sources reaching the higher interband transitions are not available. Nevertheless, one still needs to be able to detect the corresponding 2ω signal in the UV. Unfortunately the intrinsic richness of $\chi^{(2)}$ spectra remains largely to be explored experimentally we are not aware of any attempts to measure both the real and imaginary parts of the these spectral functions as one standard does in linear optics. Also, it is well known that nonlinear optical properties are so sensitive to small changes in the band structure than the linear optical properties. That is attributed to the fact that the second harmonic response $\chi_{ijk}^{(2)}(\omega)$ contains 2ω resonance along with the usual ω resonance. Both the ω and resonances can be further separated into inter-band and intraband contributions. The structure in $\chi_{ijk}^{(2)}(\omega)$ can be understood from the structures in $\epsilon_2(\omega)$. Our calculations in $ABO_3$ for $\epsilon_2(\omega)$ provides two fundamental oscillator bands at ~6 and ~10 eV which correspond to the optical transitions from the valance bands to the conduction band, formed by the d orbits of the B (Ti,Nb,Ta) atoms and consisting of two subbonds. It is well known that the $\epsilon_2(\omega)$ function computed from moments ( $\vec{p}$ ) appear to be very sensitive to the ab initio parameters and seem to be particularly appropriate to test electronic band structure. In $ABO_3$ perovskites the two peaks present in experimental reflectivity data are obtained in theoretical curves only when the interband transition moments varied with respect to the energies and $\vec{k}$ wave vectors. In this computation on $ABO_3$, compounds many parameters have been borrowed from existing computations have been neglected, explaining some discrepancies between theory and experiments [9-10, 30-35]. The structure 2-6 eV in $\chi_{ijk}^{(2)}(\omega)$ is associated with interference between a ω and 2ω resonances, while the structure above 6 eV is due to mainly to ω resonance. In Fig. 1-5 we show the 2ω interband and intraband contributions for $ABO_3$ compounds. Also given is their decomposition into intra- and interband contributions. They are

arranged so as to move the Ba → K → Li, Ti → Nb → Ta trends obvious. For example $\chi^{(2)}$ obviously increases when going from Ba to K and Li and from Ti to Nb. Unfortunately, the agreement between theory and experiment is by no means perfect [36].

Note that the interband part are negative in all cases and in most cases largely compensate the intraband part. The exceptions are the $LiBO_3$ (B=Nb,Ta) compounds in both cases of which interband part is much smaller in magnitude than the intraband part. This is quite interesting because it is unexpected. It rises the question what features in the band structure of these two compounds distinguish them from the other compounds [37, 38]. Recently, in ref.[39] were computed $A_i$ (i=1,2) and E phonon modes and nonlinear optical susceptibilities for $LiNbO_3$. Knowledge of these modes can be relevant for further theoretical EO studies. We investigated the reasons for the cancellation of intra- and interband parts by inspecting the corresponding frequency dependent imaginary parts of the $\chi^{(2)}$ (-2ω,ω,ω). First of all, one now sees that the opposite sign of intra- and interband parts not only occurs in the static value but occurs almost energy by energy. This is true over the entire energy range in $BaTiO_3$ and over most of the range (E >1 eV) for other $ABO_3$. The sign of the inter and intraband part are difficult to understand *a- priori* because a variety of matrix element products comes into play and both ω and 2ω resonances occur in both the pure interband, and the interband contribution modified by intraband motion when these are further worked out into separate resonance terms. The spectra $\epsilon_2(\omega)$ for the $ABO_3$ compounds are rather similar. They look like the superposition of the spectra of more or less four pronounced oscillators with resonance frequencies close to the M and Z line structures appearing in the 2ω and ω – terms of the imaginary parts. As an example of such a prediction the SHG coefficients of ABO3 and $A^5B^6C^7$ compounds are given in Table 2. For incident light with a frequency small compared to the energy gap. The independent tensor components are listed for ω=0. The comparison with recent experimental values and theoretical calculations [40] are also rather successful where available for the static SHG coefficients of the $ABO_3$ and $A^5B^6C^7$ compounds.

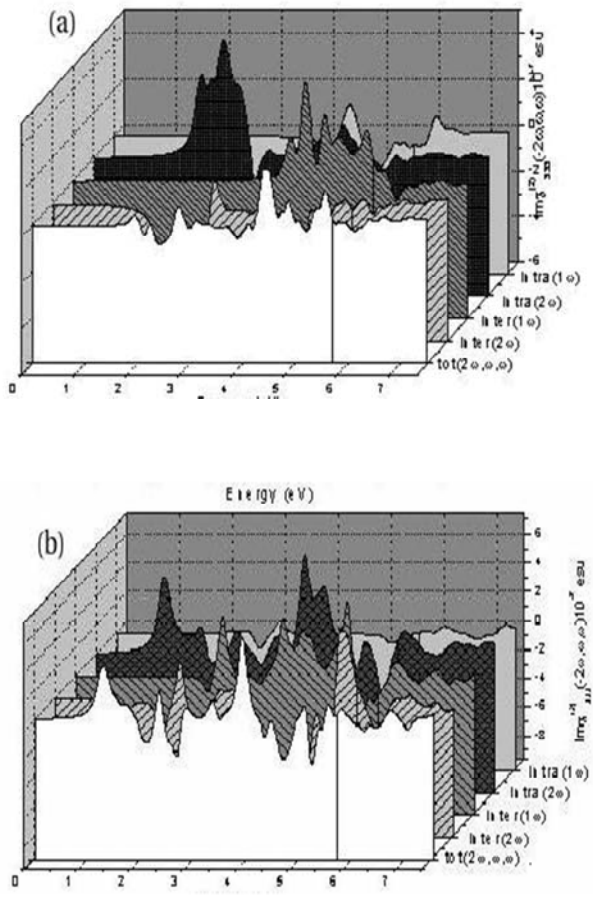


Fig. 1: Second-order susceptibility $\mathrm{Im}\,\chi^{2}_{333}(-2\omega,\omega,\omega)$ for tetragonal $LiNbO_3$ (a) and $KNbO_3$ (b)

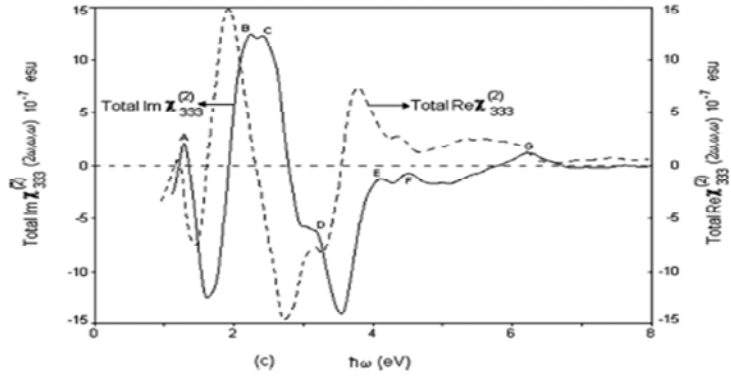


Figure 2. Second order susceptibility $\chi_{333}$ in ferroelectric phase of SbSI.

## 5. Conclusion

The linear and nonlinear optical properties for important group of ferroelectrics like $ABO_3$ ($LiNbO_3$, $LiTaO_3$, $KNbO_3$ and $BaTiO_3$) and $A^5B^6C^7$ have been calculated over a wide energy range. We studied some possible combination of A and B. This allowed us to study the trends in the second order optical response with chemical composition. The results for the zero-frequency limit of second harmonic generation are agreed to the available experiment results. The calculated linear electrooptical coefficients for $LiNbO_3$, $LiTaO_3$, KNbO3 and $BaTiO_3$ are also show agreement with recent experimental data in the energy region below band gap. For all the considered compounds the SHG coefficient $\chi^{(2)}$ is of the order of $\sim 10^{-7}$ esu. Our calculation of the SHG susceptibility shows that the intra-band and interband contributions have significantly changes with the change of B and A – ions.

## Acknowledgement

The author is grateful to ABINIT group for their ABINIT project that we used in our computations.

## References


[1] V. G. Dmitriev, D. N. Gurzadyan, D. N. Nikogosyon, *Handbook of Nonlinear Optical Crystals,* Springer-Verlag, Berrin (1991)

[2] H. S. Nalwa (ed.), *Handbook of Advanced Electronic and Photonic Materials and Devices*, Academic, San Diego (2001).

[3] P. Hohenberg, W. Kohn, Phys. Rev. **136** (1964) 864

[4] F. Bechstedt , Adv. Solid State Phys. **32** (1992) 161

[5] B. Adolph, V. I. Gavrilenko, K. Tenelsen, F. Bechsted, Phys. Rev. B **53** (1996) 9797

[6] M. Veithen., X. Gonze, Ph. Ghosez,. Phys. Rev. B **66** (2002) 235113

[7] M. Veithen, X. Gonze, Ph. Ghosez, Phys. Rev. Lett. **93** (2004) 187401

[8] X. Gonze, J-M Benken et al, Comp. Mat. Sci. **25** (2002) 478

[9] S. Cabuk, H. Akkus, A.M. Mamedov, Physica B **394** (2007) 81

[10] S. Cabuk, Optoelectronics and Adv. Mater. Rapid Commun. **1** (2007) 100

[11] R. Cohen, H. Krakauer, Phys. Rev. B **42** (1990) 6416

[12] M. Fuch, M. Scheffler, Comput. Phys. Commun. **119** (1999) 67

[13] N. Troullier, J.L. Martins, Phys. Rev. B **43** (1990) 1993

[14] J. P. Perdew, Y. Wang, Phys. Rev.B **45** 13244 (1992)

[15] D. M. Ceperley, B. J. Alder, Phys. Rev. Lett. **45** (1980) 566

[16] H. J. Monkhorst, J. D. Pack, Phys. Rev. B **140** (1976) A1333

[17] S. C. Abrahamas, J. M. Reddy, J. L. Benstein, J. Phys. Chem.Solids **27** (1966) 997

[18] S. C. Abrahamas, E. Buehler, W. C. Hamilton, S. J. Laplaca, J. Phys. Chem. Solids **34,** (1973) 521

[19] http://cst-www.nrl.navy.mil.

[20] A. W. Hewat, J. Phys. C: Solid State Phys. **6** (1973) 2559

[21] G. H. Kwei, A. C. Lawson, S. J. L. Bilinge, S-W. Cheong, J. Phys. Chem. **97** (1993) 2368

[22] E. Ghahramani, J.E. Sipe, Phys. Rew. B 46 (1992) 1831

[23] W. G. Aulbur, L. Jonsson , J. W. Wilkins, Solid State Physics **54** (2000) 1

[24] W. R. V. Lambrecht, S. N. Rashkeev, Phys. Stat. Sol (b) **217** (2000) 599

[25] A. H. Reshak, Eur. Phys. J. B **47** (2005) 503

[26] V. L. Gavrilenko, Phys. Stat. Sol (a) **188** (2001) 1267

[27] M. Zgonik, P. Bernasconi, M. Duelli, R. Schlesser, P. Günter, Phys. Rev. B **50,** 5941 (1994)
[28] A. Rauber, *in Current Topics in Materials Science*, edit by E. Kaldis North-Holland Publishing Company (1978)
[29] R. W. Boyd, *Nonlinear Optics*, Academic Press, Inc., (1992)
[30] A. M. Mamedov, L. S. Gadzhieva, Sov. Phys. States **26** (1984) 1732
[31] A. M. Mamedov, M. A. Osman, L. C. Hajieva, Appl. Phys. A **34** (1984) 189
[32] A. M. Mamedov, Opt. Spektroc. **56** (1984) 645
[33] M. Veithen, X. Gonze, Ph. Ghosez, Phys. Rev. B **65** (2002) 214302
[34] M. Veithen, X. Gonze, Ph. Ghosez, Phys. Rev. B **71** (2005) 125107
[35] X. Y. Meng, Z. Z. Wang, Y. Zhu, C. T. Chen, J.Appl. Phys.**101** (2007) 103506
[36] D. Xue, S. Zhang, Phil. Mag. B **78** (1998) 29
[37] D. Xue, K. Betzler, H. Hesse, Optical Materials **16** (2001) 381
[38] D. Xue, S. Zhang, J.Phys.Solids **58,** 1399 (1997)
[39] P. Hermet, M. Veithen, Ph. Ghosez, J. Phys.:Condens. Matter **19** (2007)456202
[40] D. Xue, S. Zhang, Chem. Phys. Lett. **291** (1998) 401
[41] M. J. Weber, *Handbook of Optical Materials*, CRC press (2003)